ELSEVIER

PII: S0032-3861(97)00611-3

Polymer Vol. 39 No. 13, pp. 2977–2981, 1998

0032-3861/98/$19.00+0.00

Solubilization of *n*-alkanes into polyazomethines having flexible (*n*-alkyloxy)methyl side chains: 2. Theoretical model for the estimation of solubility limit

Heesub Kim, Hwan-Koo Lee and Wang-Cheol Zin*

Department of Materials Science and Engineering, Pohang University of Science and Technology, San 31, Hyoja-dong, Nam-ku, Pohang, 790-784 Kyungbuk, South Korea

(Received 27 June 1996; revised 11 November 1996; accepted 7 January 1997)

In a previous paper (H. Kim et al., *Polymer*, 1996, 37, 2573), the solubility limit of *n*-alkanes in blends of *n*-alkane/polyazomethine having flexible (*n*-alkyloxy)methyl side chains was reported as a function of side chain lengths of the polymer and chain lengths of *n*-alkanes. This paper proposes a theoretical model for estimating the solubility limit of *n*-alkanes. The model assumes that *n*-alkanes solubilize only into the layered side chain domain and that the side chain has a hyperbolic tangent function profile due to very high grafting density and density uniformity. The calculated solubility limit of *n*-alkane increases and decreases with increasing chain length of the side chain and chain length of the *n*-alkane, respectively. The model predictions are in qualitative agreement with experimental results (H. Kim et al., *Polymer*, 1996, 37, 2573) although the former are much lower than the latter.

(Keywords: polyazomethine; *n*-alkane; solubility limit)

INTRODUCTION

Recent literature [2–8] contains a number of reports on rigid-rod polymers with flexible side chains. Increasing the amount of substitution or the length of the side chains results in a lower melting point and a better solubility. Furthermore, flexible side chains lead to the formation of novel layered structures in the crystalline phase and mesophase. In the layered structures, stiff main chains form backbone layers and flexible side chains emanating from the layers fill the space between the layers. The phase behaviour of these rigid-rod polymers is mainly governed by the strong segregation of aromatic main chains from aliphatic side chains, being analogous to microphase separation in block copolymers.

In a previous paper[1], the solubilization behaviour of *n*-alkanes (C_k, $k = 15, 20, 32, 40$ and 50) into polyazomethines (C_m-PAM) with flexible (*n*-alkyloxy)methyl side chains ($CH_2OC_mH_{2m+1}$, $m = 4, 6, 9, 12$) was studied by measuring layer spacings of the layered structures by means of wide-angle X-ray scattering (WAXS) and the solubility limit of the *n*-alkanes were evaluated as a function of side chain lengths of the polymers and the chain lengths of the *n*-alkanes. With increasing side chain length of C_m-PAM and chain length of C_k, the solubility limit of *n*-alkane increased and decreased, respectively. Similar phenomena have been investigated in many binary blends of A homopolymer/AB block copolymer[9–13]. Contrary to the case of block copolymers, however, the grafting density of the side chains of C_m-PAM is very high (0.33) and is not changed by addition of *n*-alkane. Hence, theories developed for block copolymers need a modification in order to be applied to this system.

In this paper, we use Meier's confined-chain model[9] for estimating the solubility limit of mobile molecules, e.g. *n*-alkanes, in blends of mobile molecules and rigid-rod polymers having flexible side chains, e.g. the polyazomethine. We believe that Meier's model, although approximate, makes the contributions to the free energy change by various physical factors more intuitively. Since the density profile of the side chain is different from that of the block copolymer due to the very high grafting density of the side chain, we assume the hyperbolic tangent density profile for the side chain, which is suggested for a polymer brush by Shull[14,15]. The results obtained from this model are compared with those of the experimental investigations[1].

MODEL AND ASSUMPTIONS

Figure 1a shows schematic diagram of the layered mesophase of a rigid-rod polymer with flexible side chains. The main chains form the backbone layer and molten side chains fill the space between the backbone layers. The side chains are regularly grafted to the backbone layer and the grafting density of the side chain is very high. Due to the fixed grafting density, there is a linear relationship between the layer spacing and the side chain length. *Figure 1b* shows a schematic diagram of the layered structure on mixing of the mobile chain and rigid-rod polymer with flexible side chains. Mobile chains having a chemically similar structure to the side chains are miscible with the side chains and solubilize into side chain domains, thereby increasing the layer spacing between backbone layers. The grafting density of the side chain is not changed on mixing.

Before the calculation of the free energy change on mixing, the density profile of the side chain should be determined since the free energy change greatly depends on

* To whom correspondence should be addressed

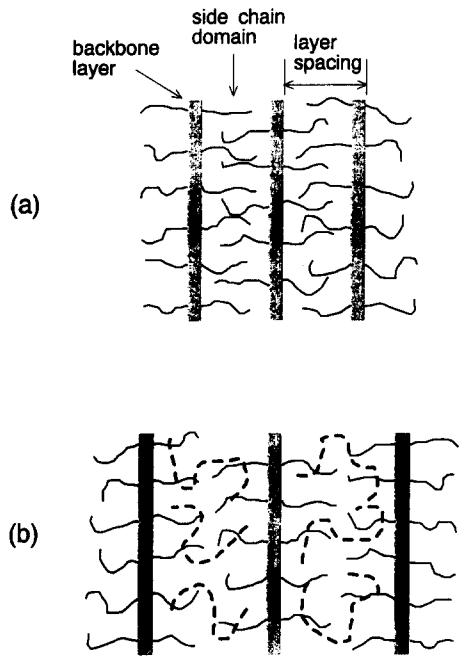

Figure 1 Schematic diagram for mixing of mobile chain and rigid-rod polymer having flexible side chains in the layered mesophase. (a) Pure rigid-rod polymer having flexible side chains; (b) blend of mobile chain and rigid-rod polymer having flexible side chains. Mobile chains are indicated by the dotted lines

the density profile of the side chain. The side chain grafted to the backbone layer is analogous to the polymer brush[14–18] which is grafted to an inert flat surface. According to the studies on polymer brushes, they have density profiles close to a step function in the case of very high grafting densities. Furthermore, in the case of two interacting brushes grafted to opposite surfaces, the total density which is the sum of the density of each brush density should be uniform. Considering the high grafting density of the side chain and the density uniformity, we are led to assume a hyperbolic tangent function profile for the side chain, which is suggested for polymer brushes by Shull[14,15].

Density profile of the side chain in a pure state

Figure 2a shows the density profile of the side chain in the side chain domain, where d is the layer spacing and d_{S0} is the thickness of the domain to which the side chain is confined and d_M is the thickness of the main chain domain. The horizontal axis denoted by x indicates the distance across the domains and the vertical one denoted by $\rho_S(x) = \rho_{SL}(x) + \rho_{SR}(x)$. The two components are given by

$$\rho_{SL}(x) = \frac{1}{d}\left(\frac{1}{2} - \frac{1}{2}\tanh\left(\frac{px}{d_{S0}} - \frac{p}{2}\right)\right) \quad (1)$$

$$\rho_{SR}(x) = \frac{1}{d}\left(\frac{1}{2} - \frac{1}{2}\tanh\left(\frac{p(d_S - x)}{d_{S0}} - \frac{p}{2}\right)\right) \quad (2)$$

where, p is a variable which determines the density profile and $\rho_{SL}(x)$, the reduced density of the left side chain defined as $\int_0^{d_{S0}} \rho_{SL}(x)dx = (f_S)/2$ where f_S is the volume fraction of the side chain in a rigid-rod polymer with flexible side chains, and $\rho_{SR}(x)$, the reduced density of the right side chain, is defined similarly. The side chain will have a maximum entropy when it has a step function profile. Therefore, the side chain at pure state is assumed to have a profile very close to a step function as shown in *Figure 2a*.

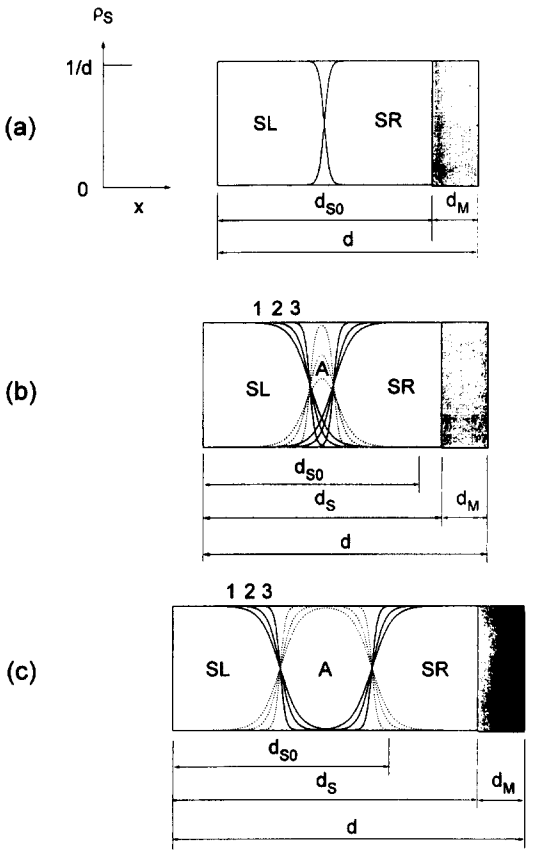

Figure 2 Schematic diagram for the density profile on mixing of mobile chains and side chains. A, SL and SR denote mobile chain, left side chain and right side chain, respectively. d is the layer spacing, d_{S0} is the thickness of the domain to which the side chain is confined, d_M is the thickness of the main chain domain, and d_S is the thickness of the domain which contains both the side chain and the mobile chain: (a) pure side chain; (b) mobile chain + side chain. As an example of the change in the density profile of the side chain on mixing, three forms of density profiles denoted by numbers 1, 2, and 3 are given. In the sequence of increasing numbers, p increases; (c) mobile chain + side chain. On further addition of mobile chain, pure mobile phase is formed

Density profile of side chain in a mixed state

Figure 2b and *c* show the density profile for a side chain mixed with a mobile chain where d_S indicates the thickness of the domain which contains both the side chain and the mobile chain. The total density, $\rho_t(x)$, is composed of the side chain and mobile chain densities as shown in *Figure 2b* and *c*: $\rho_t(x) = \rho_S(x) + \rho_A(x)$. Since the grafting density which is very high is not changed on mixing, the density profile of the side chain in the mixed state will also have a hyperbolic tangent form. Hence, the thickness to which the side chain is confined will not be changed on mixing.

The free energy change on mixing of the mobile chain and side chain is estimated by the model including the localized solubilization of added mobile chains, where the mobile chains are not distributed uniformly throughout the microdomain space but are localized in the central part of it. *Figure 2b* and *c* show the localization of the added mobile chain in the central part of the side chain domain and also show the variation of the density profile in the side chain domain which is a function of p. When mobile chains are mixed with side chains, the density profile of the side chain may be changed and therefore p can have a different value at a given volume fraction of mobile chain as marked by 1, 2, 3. Hence the equilibrium density profile which gives

the lowest free energy change on mixing should always be determined at a given volume fraction of mobile chains.

Free energy change on mixing

The free energy change associated with adding a mobile chain to the side chain is given by

$$\Delta G_{mix} = \Delta H_{mix} - T(\Delta S_{confS} + \Delta S_{confA} + \Delta S_{trans} + \Delta S_{elas}) \quad (3)$$

The first term on the right-hand side in equation (3), ΔH_{mix}, indicates the enthalpy change of mixing. Since the mobile chains are chemically similar to the side chains, the enthalpy change will be negligible and can be assumed to be zero. The first term in parentheses is the conformational entropy change of the side chain associated with the addition of mobile chain. The second term is the conformational entropy losses due to the compression of the mobile chain in the side chain domain. The third term is the translational entropy change of the mobile chain on mixing the mobile chain and side chain. The last term is the elastic entropy change of the side chain, which comes from the variation of its end-to-end distance compared to that of the pure side chain.

MATHEMATICAL FORMULATION

On the basis of the density profile as shown in *Figure 2*, the contribution of each of four terms to the free energy change (equation (3)) can be formulated.

Conformation entropy change of the side chain

The conformational entropy change per unit volume of the side chain confined within the layers of thickness of d_{S0} is given by[9,19]

$$\Delta S_{confS} = \frac{R\Phi_S}{V_S}\ln P_S^1(d_{S0}; d_1) - \frac{R\Phi_S}{V_S}\ln P_S^0(d_{S0}; d_1) \quad (4)$$

$$P_S^0(d_{S0}; d_1) = \frac{4d_{S0}}{\pi^2 d_1}\sum_{n=1,3,\ldots}^{\infty}\frac{1}{n^2}\left(1 - \cos\frac{n\pi d_1}{d_{S0}}\right) \times \exp\left[-\frac{n^2\pi^2 N_S b_S^2}{6d_S 0^2}\right] \quad (5)$$

where R is the gas constant, V_S the molar volume of the side chain, Φ_S the volume fraction of the side chain satisfying the condition $\Phi_S + \Phi_M + \Phi_K = 1$ where Φ_M is the volume fraction of the main chain and Φ_K is the volume fraction of mobile chain, P_S^0 the probability of the pure side chain that the grafted end point is anywhere within the interface between the main chain and side chain and the free end point is anywhere within the layers of thickness d_{S0}, P_S^1 the similar probability of the side chain in the mixed state, d_1 the interfacial thickness between the main chain and the side chain, N_S the number of statistical elements (monomer units) of the side chain, and b_S the length of statistical elements (monomer units) of the side chain. Since the probabilities are independent of the change in the density profile, that is, the change in p value, P_S^1 is equal to P_S^0, and hence this entropic contribution is equal to zero.

Conformational entropy change of the mobile chain

The conformational entropy change per unit volume of the mobile chain confined within the layers of thickness of d_S is given by[9,19]

$$\Delta S_{confA} = \frac{R\Phi_K}{V_K}\ln\left(\frac{8}{\pi^2}\sum_{n=1,3,\ldots}^{\infty}\frac{1}{n^2}\exp\left[-\frac{n^2\pi^2 N_K b_K^2}{6d_S^2}\right]\right) \quad (6)$$

where V_K is the molar volume of the mobile chain, and N_K is the number of statistical elements (or monomer units) of length b_K.

Since the added mobile chain is to be dissolved only into the side chain domain, the increment of layer spacing due to volume change can be calculated from a geometrical consideration[20]. The thickness of the side chain domain increased by addition of mobile chain is given by

$$d_S = \frac{(1-\Phi_K)f_S + \Phi_K}{(1-\Phi_K)(1-f_S)}d_M \quad (7)$$

Translational entropy change of mobile chain

Since the layered structure in the mesophase can be thought of as a kind of network, the translational entropy change on mixing for the rigid-rod polymer with flexible side chains seems to be negligible, and hence in our study the entropy change for only the mobile chain is considered.

The translational entropy change per unit volume for the mobile chain can be obtained by integration

$$\Delta S_{trans} = \frac{R}{V_K}\int_0^{d_S}\rho_K(x)\ln\frac{\rho_K(x)+\rho_S(x)}{\rho_K(x)}dx \quad (8)$$

where $\rho_K(x)$ is the reduced den-sity of the mobile chain defined as $\int_0^{d_S}\rho_K(x)dx = \phi_K$ and $\rho_S(x)$, the reduced density of the side chain, is defined as $\int_0^{d_{S_0}}\rho_S(x)dx = \phi_S$.

Elastic entropy change of the side chain

The density profile of the side chain is variable as shown

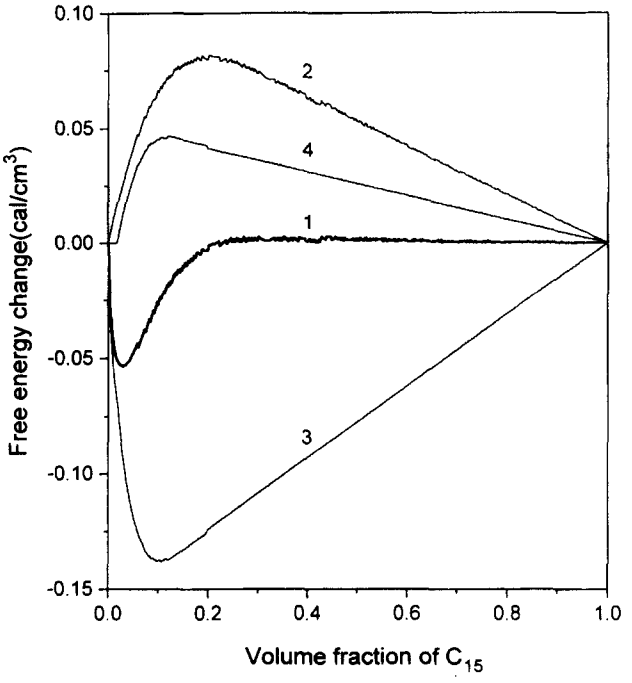

Figure 3 The free energy change of C_{15}/C_8-PAM blend as a function of the volume fraction of C_{15}, calculated at 180°C. Curve 1 - the total energy change. Curve 2 - the energy change by the conformational entropy change of C_{15}. Curve 4 - the energy change by the elastic entropy change of the side chain

in *Figure 2b* and *c*, which brings about the change in the end-to-end distance of the side chain. The elastic entropy change of the side chains per unit volume can be formulated as follows[19,21] (for 1-dimension)

$$\Delta S_{elas} = -\frac{1}{2}R\frac{\Phi_S}{V_S}(W_1^2 - 1 - 2\ln W_1) + \frac{1}{2}R\frac{\Phi_S}{V_S}(W_0^2 - 1 - 2\ln W_0) \quad (9)$$

$$W_0 = \frac{\sqrt{\overline{x_{side}^2}}}{\sqrt{\overline{x_{free}^2}}} \quad (10)$$

where, W_0 is the ratio of the end-to-end distance of the side chain to that of the free chain which has the same chemical structure with the side chain in the pure state, and W_1 is defined similarly in the mixed state. The value of the free chain's end-to-end distance ($\sqrt{\overline{x_{free}^2}}$) can be obtained from the characteristic ratio of the free chain which has the same chemical structure as the side chain. The side chain's end-to-end distance was approximated by

$$\sqrt{\overline{x_{side}^2}} = \sqrt{\frac{\int_0^{d_{S0}} x^2 x \frac{\partial \rho_{SL}(x)}{\partial x} dx}{\int_0^{d_{S0}} x \frac{\partial \rho_{SL}(x)}{\partial x} dx}} \quad (11)$$

COMPARISON OF SOLUBILITY LIMIT WITH EXPERIMENT

For the calculation of the free energy change on mixing of *n*-alkanes and C_m-PAM, d_{S0} and f_S values in equation (1) and

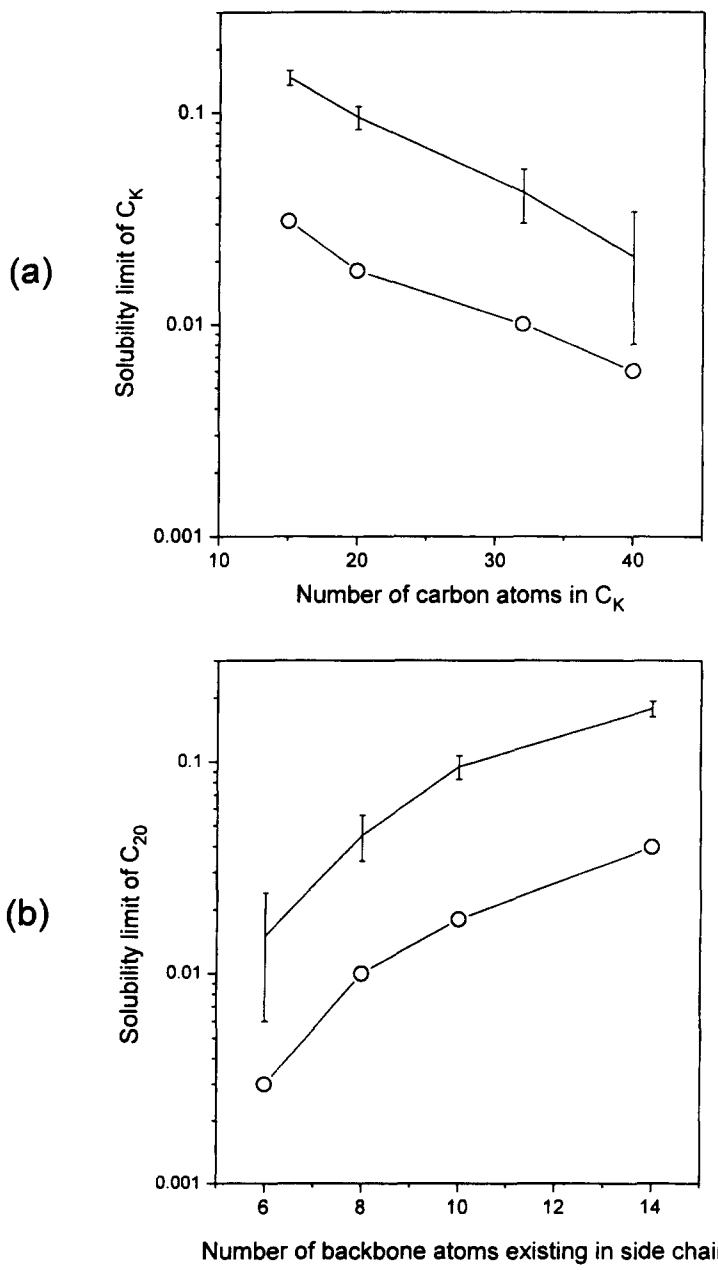

Figure 4 (a) Comparison of solubility limit between experimental (denoted as bar) and theoretical values (denoted as open circle) in C_k/C_8-PAM blend as a function of the number of carbon atoms in the *n*-alkane. (b) Comparison of the solubility limit between experimental and theoretical values in C_{20}/C_m-PAM blend as a function of the number of backbone atoms in the side chain

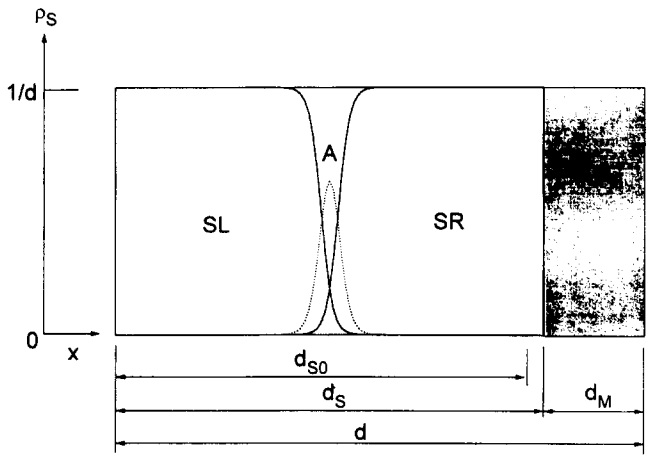

Figure 5 Schematic diagram for the actual density profile for C_{20}/C_{12}-PAM blend at its theoretical solubility limit. The notations have the same meaning as those in *Figure 2*

equation (2), and the b_K value in equation (6), and the $\sqrt{x_{free}^2}$ value in equation (10) should be determined. As mentioned in the previous paper[1], d_M is about 4.8 Å and may be assumed not to change with side chain length of C_m-PAM or on blending *n*-alkane. With this d_M value, d_{S0} and f_S values were obtained using layer spacing (d value) from the previous experiment[1]. Although the characteristic ratio is a function of chain length and temperature[22], for simplicity, the approximate values of b_K and $\sqrt{x_{free}^2}$ values were obtained assuming that the characteristic ratio is fixed to 2, irrespective of the chain length or the temperature for all C_k/C_m-PAM blends. As a representative example of the free energy change on mixing, the free energy change for C_{15}/C_8-PAM blend was obtained as shown in *Figure 3* as a function of volume fraction of C_{15} calculated at 180°C. The individual contributions were calculated using equation (6), equation (8), and equation (9), respectively. As seen from *Figure 3*, the translational entropy change of the *n*-alkane tends to make mixing favourable, whereas the conformational entropy change of the *n*-alkane and the elastic entropy change of the side chain tend to make it unfavourable. The solubility limit is determined by the volume fraction of *n*-alkane whose chemical potential is equal to that of the pure *n*-alkane.

Figure 4a and *b* show comparisons of the solubility limit between the current model predictions and the experimental results for C_k/C_m-PAM blend as a function of the length of C_k and the side chain length, respectively. The current model predicts that the solubility limit increases and decreases with increasing side chain length and chain length of *n*-alkane, respectively. These predictions, however, are only in qualitative agreement with experimental results.

It is interesting to examine the equilibrium density profile of the side chain and mobile chain on mixing. As an example, *Figure 5* shows the actual density profile for C_{20}/C_{12}-PAM blend at its theoretical solubility limit. It is found that the system does not incorporate sufficient mobile phase to form a separate pure mobile phase region at its theoretical solubility limit.

This model can be applied to such general layered mesophases having very high grafting densities as other rigid-rod polymers having flexible side chains or rod-coil polymers which have a layered mesophase. It is hoped that our results will stimulate more rigorous analysis of this interesting problem.

ACKNOWLEDGEMENTS

This work was supported by the Korea Science and Engineering Foundation (95-0501-08-01-3).

REFERENCES

1. Kim, H., Jung, J.C. and Zin, W.-C., *Polymer*, 1996, **37**, 2573.
2. Ballauff, M., *Makromol. Chem. Rapid Comm.*, 1986, **7**, 407.
3. Rodriguez-Parada, J.M., Duran, R. and Wegner, G., *Macromolecules*, 1989, **22**, 2507.
4. Stern, R., Ballauff, M., Lieser, G. and Wegner, G., *Polymer*, 1991, **32**, 11.
5. Watanabe, J., Harkness, B.R., Sone, M. and Ichimura, H., *Macromolecules*, 1994, **27**, 507.
6. Kriecheldorf, H.R. and Domschke, A., *Macromolecules*, 1994, **27**, 1509.
7. Park, S.-B., Kim, H., Zin, W.-C. and Jung, J.C., *Macromolecules*, 1993, **26**, 1627.
8. Kim, H., Park, S.-B., Jung, J.C. and Zin, W.-C., *Polymer*, 1996, **37**, 2845.
9. Meier, D.J., *Polym. Prepr.*, 1977, **18**, 340.
10. Tanaka, H., Hasegawa, H. and Hashimoto, T., *Macromolecules*, 1991, **4**, 240.
11. Winey, K.I., Thomas, E.L. and Fetters, L.J., *Macromolecules*, 1991, **24**, 6182.
12. Kang, C.-K. and Zin, W.-C., *Macromolecules*, 1992, **25**, 3039.
13. Semenov, A.N., *Macromolecules*, 1993, **26**, 2273.
14. Shull, K.R., *J. Chem. Phys.*, 1991, **94**, 5723.
15. Shull, K.R., *Macromolecules*, 1996, **29**, 2659.
16. de Gennes, P.-G., *Macromolecules*, 1980, **13**, 1609.
17. Murat, M. and Grest, G. S., *Computer Simulation of Polymers*. ed. R. J. Roe. Prentice Hall, 1991, Chap. 10.
18. Fleer, G. J., Cohen Stuart, M. A., Scheutjens, J. M. H. M., Cosgrove, T. and Vincent, B., *Polymers at Interfaces*. Chapman and Hall, London, 1993, Chap. 8.
19. Lee, H.-K., Kang, C.-K. and Zin, W.-C., *Polymer*, 1996, **37**, 287.
20. Skoulios, A. E., *Developments in Block Copolymers*. ed. I. Goodman. Applied Science Publishers, London, 1982, Chap. 3.
21. Meier, D.J., *J. Polym. Sci.: Part C*, 1969, **26**, 81.
22. Flory, P. J., *Statistical Mechanics of Chain Molecules*. Interscience Publishers, New York, 1969, Chap. 5.